Mechanical Systems and Signal Processing 164 (2022) 108293

Contents lists available at ScienceDirect

Mechanical Systems and Signal Processing

journal homepage: www.elsevier.com/locate/ymssp

Damage identification of tube bundles with crack subjected to cross-flow and loose support

Lingling Lu [a,b], Jiang Lai [c,*], Shihao Yang [c], HW Song [a,b], Lei Sun [c]

[a] Key Laboratory for Mechanics in Fluid Solid Coupling Systems, Chinese Academy of Sciences, Institute of Mechanics, Beijing 100190, China
[b] School of Engineering Science, University of Chinese Academy of Sciences, Beijing 100049, China
[c] Nuclear Power Institute of China, Chengdu 610213, China

ARTICLE INFO

Keywords:
Damage identification
Baseline-free
Nonlinear dynamics
Tube bundles
Two-phase flow

ABSTRACT

Dynamic characteristics of tube bundles with crack subjected to cross-flow and nonlinear loose support are very complicated, making the damage identification more difficult, and the information of healthy tube bundles could not be used in the damage identification process. In this paper, a baseline-free damage detection method is proposed to detect the crack damage of tube bundles subjected to cross-flow and loose support. Two damage indexes, based on the root mean square value of structural vibration responses and the gapped smoothing method, are proposed to identify the damage location and damage extent. Cases with different damage locations and damage extents are considered. The influences of the flow pitch velocity, loose support and the number of measure points on the effectiveness of the method are also discussed. The results showed that the index based on the normalized values of root mean square displacement and velocity responses can identify the damage location accurately within the flow pitch velocity range considered in this study. An improved index based on the normalized values of root mean square displacement and velocity responses and a parameter reflecting damage extent can identify the damage extent when the flow pitch velocity is small. When the flow pitch velocity is large, the effectiveness of the improved index is affected. Meanwhile the loose support location also has an influence on the proposed method, especially when the flow pitch velocity is large. Number of measure points has little influence when the damage extent is larger than 5%.

1. Introduction

Tube bundles in many industrial components such as steam generators and heat exchangers are subjected to several types of flow-induced excitations: turbulence buffeting, vortex shedding, and fluidelastic instability. Fluidelastic instability is the most important mechanism. When the flow pitch velocity exceeds a critical value, the fluidelastic instability may occur, resulting excessive collision between the tube bundles and the support structures that may lead to the tube damage [1]. Once the tube bundles' damages emerge, the safety of a nuclear power plant will be a great challenge. Since the 1960 s, a great effort has been dedicated to this flow-induced vibration of heat exchangers [2,3]. However, there is little work on damage identification of the flow-induced vibration tube bundles with damages. The collision makes the tube bundles system exhibit complex responses containing harmonic distortion, jumps, modal interactions, bifurcation and possible chaos [4], causing the damage identification more difficult.

* Corresponding author.
E-mail address: laijiang1983@163.com (J. Lai).

https://doi.org/10.1016/j.ymssp.2021.108293
Received 20 February 2021; Received in revised form 19 June 2021; Accepted 28 July 2021

Available online 6 August 2021

Damage detection technology for structures can be classified into two categories: linear elastic method and nonlinear dynamic approach [5]. The linear elastic method can be sub-categorized as the modal method [6-8] and the wave motion method. Most of the research methods in the damage detection are limited to or based on the theory of linear dynamics. However, in practice, some typical sources of nonlinearity are geometric nonlinearities, gaps, bolted connections, clearance, impacts, cracks, materials with nonlinear constitutive relationship, and so on [9]. As a consequence, even simple systems can exhibit complex nonlinear responses containing harmonic distortion, jumps, modal interactions, bifurcation, and chaos [10]. Many developed damage identification methods are based on the linear elastic theory. When there are nonlinear factors, those factors will reduce the effectiveness of the proposed methods or make those methods failure. A few literatures relate to the nonlinear theory, such as the stochastic analysis [11,12], the wavelet transform [13], the worm transform [14], the Hilbert-Huang transform [15] and so on.

The previous works dealing with nonlinear structures can be divided into two types. For the first one, the system is considered to be linear and the damage induced a nonlinearity of structural responses [16]. The identification of structural damage can be treated as a procedure for the detection of nonlinearities in the measured structural responses. Many methods have been developed [17,18]. For the second type, the system is considered to be nonlinear before the occurrence of the damage [19]. It needs to model the baseline behavior of the structure in a way that the inherent nonlinear effects of the system are not mistakenly viewed as damage [9].

Shiki et al. [9] proposed a discrete Volterra model to monitor the prediction error of a reference model representing the healthy structure. The model could separate the linear and nonlinear components of the response of a system. Jiang et al. [20] employed proper orthogonal decomposition to establish a damage location method for beam-like structures. By comparing the nonlinearity degrees of the characteristic points in undamaged and damaged structures, the location was identifiable by finding the positions of maximal change. Luis et al [21] proposed a detection method based on a nonlinear stochastic index and hypothesis test, considering different levels of simulated damage, associated with loss of mass. By using the time–frequency analysis with this appropriate moving window width, Wang et al. [5] used the relationship between displacement amplitude and corresponding natural vibration frequency at different damage levels in the case of free vibration to depict and analyze the damaged RC beam. The proposed method may be suitable for structures with damage invisible or hard to be found by naked eyes. Bhowmik et al. [22] used recursive canonical correlation analysis for robust damage detection of the linear and nonlinear systems. The method generates proper orthogonal modes at each time stamp and is applied on the combined ambient and earthquake responses obtained from the UCLA Factor Building, verifying the proposed method an ideal candidate for real time Structural Health Monitoring.

In this study, a baseline-free damage identification method is proposed to identify the damage location in the tube bundles subjected to cross-flow and loose support. The cubic spring model is used to simulate the loose support. Effectiveness of the proposed method on detecting damage location and extent are discussed. Besides, the influences of many factors on the method, such as the flow pitch velocity, loose location, number of measure points, are discussed.

2. Mathematical model and damage identification methodology

In this section, the mathematical model is presented briefly and the damage identification method is introduced in detail.

2.1. Brief introduction of the mathematical model

In our previous studies [1], considering the effect of the fluidelastic force, a mathematical model of a flexible tube in a rotated triangular tube array with loose support was presented. Based on this model, the effect of the flow pitch velocity on the fluidelastic instability and post-instability were investigated. The flow pitch velocity, U_p, can be calculated from the free stream velocity, U_∞, as:

$$U_p = \frac{P}{P-D}U_\infty \tag{1}$$

where D is the tube diameter, P is the pitch between the tube bundles.

However, it should be noted that when there is a damage in a tube, the vibration characteristics of the tube could change a lot compared with the tube without damage. Thus, in our another submitted paper, a mathematical model of a flexible tube in a rotated triangular tube array with a crack subjected to cross-flow and loose support was developed, and the dynamic characteristics of the tube bundles system were investigated. The model takes into account the variations of the tube natural frequency and mode of the vibration owing to the crack damage. Moreover, a cubic spring model was used to simulate the nonlinear boundary condition. A comprehensive description of this model was presented in reference [23]. In the work, explanations and values of the parameters for the model

Table 1
Explanations and the values of the parameters.

Parameters	Values
Elasticity modulus	$E = 210$ GPa
Tube density	$\rho_T = 7800$ kg/m^3
Tube length	$L = 0.312$ m
Tube outer diameter	$OD = 0.01748$ m
Tube inner diameter	$ID = 0.01544$ m
Pitch between tubes	$P = 0.0259$ m
Water density	$\beta_L = 1000$ kg/m^3

presented in reference [23] are listed. (See Table 1).

In addition, from the dynamic analysis, we found that the crack damage has a significant influence on the nonlinear vibration characteristics of the tube bundles system. The nonlinear dynamics characteristics of the tube bundles system can be summarized as follows. Firstly, the limit cycle motion of the tube bundles system may occur at a certain flow pitch velocity considering the effect of the support structures. For the cracked tube bundles system, the limit cycle motion is much more complicated. Secondly, with the flow pitch velocity increases, the effect of the support structures on the vibration responses of the cracked tube becomes more visible than those of the intact tube. The impact-sliding and several impacts between the tube and the support structure occur, during one oscillation cycle.

2.2. Damage identification method

The loose support and cross-flow make the tube bundles system vibration more complicated. As the flow pitch velocity increases, once the velocity exceeds the threshold of fluidelastic instability, three typical vibration forms: the periodic motion, quasi-periodic motion and non-periodic motion may appear. Those factors make the structural damage identification more difficult.

When there is a damage in a tube, the vibration characteristics of the tube will change compared with the tube without damage. Structural damage causes the variation of stiffness distribution, then the structural vibration property will change. When the crack damage is small, it is hard to detect it. As the damage extent increases, the variation of structural dynamic response becomes obvious as the damage accumulates. In the paper, the lateral displacement and velocity responses are used to construct the damage index for damage identification. Considering the nonlinear factors, the information of a healthy tube could not be used as the baseline, and the traditional damage identification method with baseline could not be used any more. A baseline-free damage identification method is developed for the tube bundles with strong nonlinear dynamic characteristics.

As we know, when there is a damage, it affects the distributed stiffness, mass and damping, and the variation of local stiffness around the damage is more obvious. Further, vibration information, such as mode shapes, time domain responses (displacement, velocity) will display discontinuity or singularity around the damage. Therefore, in the work, gapped smoothing method (GSM) [24,25] is used for damage identification without a baseline or healthy data. One-dimensional GSM is employed. Four neighboring points are selected to fit the value of measure point x_i, as shown in Fig. 1. The estimated y_i' could be expressed as follows,

$$y_i' = a_0 + a_1 x_i + a_2 x_i^2 + a_3 x_i^3 \tag{1}$$

where the four coefficients a_0 to a_3 could be obtained by the four points around point x_i, and are expressed as follows:

$$A_i = C_i \times Y_i \tag{2}$$

where A_i is $\{a_0, a_1, a_2, a_3\}_{4\times1}$ for the measure point x_i. C_i is the coefficient matrix for the measure point $\mathrm{x_i}$, expressed as Eq. (3). Y_i is $\{y_{i-2}, y_{i-1}, y_{i+1}, y_{i+2}\}_{4\times1}$.

$$C_i = \begin{bmatrix} 1 & x_{i-2} & x_{i-2}^2 & x_{i-2}^3 \\ 1 & x_{i-1} & x_{i-1}^2 & x_{i-1}^3 \\ 1 & x_{i+1} & x_{i+1}^2 & x_{i+1}^3 \\ 1 & x_{i+2} & x_{i+2}^2 & x_{i+2}^3 \end{bmatrix}^{-1} \tag{3}$$

The effect of damage on structure becomes obvious as the time accumulates. Root mean square (RMS) of structural responses (displacement and velocity) of measure point x_i is expressed as:

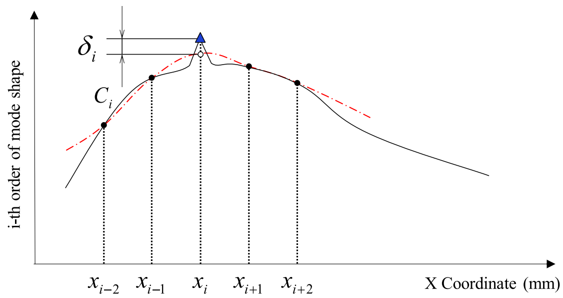

Fig. 1. One-dimensional gapped smoothing method.

$$RMSS_i = \sqrt{\left(\sum_{t=t_1}^{t_2} S_{i,t}^2\right)/M}$$
$$RMSV_i = \sqrt{\left(\sum_{t=t_1}^{t_2} V_{i,t}^2\right)/M} \tag{4}$$

where $S_{i,t}$, $V_{i,t}$ is the displacement and velocity of measure point x_i at the sampling time t respectively. t_1 and t_2 is the beginning and ending time of the sampling respectively, M is the number of sampling time points.

Based on the real values $RMSS_i$, $RMSV_i$ and the estimated values $RMSS_i$', $RMSV_i$' fitted according to Eq. (1), the absolute variation DVS_i and DVV_i of measure point x_i can be expressed as,

$$DVS_i = RMSS_i^{'} - RMSS_i$$
$$DVV_i = RMSV_i^{'} - RMSV_i \tag{5}$$

Damage index AV_i^{RMS} of measure point x_i, based on the normalized values of RMS displacement and velocity responses, is presented,

$$AV_i^{RMS} = NDV_i^S + NDV_i^V \tag{6}$$

where NDV_i^S is the normalized value of measure point x_i based on the displacement responses, and NDV_i^V the normalized value of measure point x_i based on the velocity responses. The two indexes are expressed as Eq. (7):

$$NDV_i^S = \left|(DVS_i)^2 - min(Z_S)^2)/(max(Z_S)^2 - min(Z_S)^2)\right|$$
$$NDV_i^V = \left|(DVV_i)^2 - min(Z_V)^2)/(max(Z_V)^2 - min(Z_V)^2)\right| \tag{7}$$

where Z_S is $\{DVS_1, DVS_2, \ldots\ldots, DVS_N\}$, Z_V is $\{ DVV_1, DVV_2, \ldots\ldots, DVV_N \}$, and N is the number of measure points.

According to Eq. (7), it is seen that the index NDV_i^S and NDV_i^V are from 0 to 1, therefore the range of index AV_i^{RMS} is from 0 to 2. For damages with different extents, the range of index AV_i^{RMS} is same, the proposed index can identify the damage location and it is hard to detect the damage extent effectively. An improved index RV_i^{RMS}, based on the normalized values of RMS displacement and velocity responses and a parameter reflecting damage extent, is proposed,

$$RV_i^{RMS} = RNS_i + RNV_i \tag{8}$$

where parameter RNS_i and RNV_i are calculated according to Eq. (9). α_S and α_V can be obtained according to Eq. (10). From Eq. (10), it is seen that the parameter α_S and α_V could reflect the amplitude of structural responses' variations. If the damage extent is small, then α_S and α_V is small. If the damage extent is large, α_S and α_V will be large. Therefore, index RV_i^{RMS} could reflect the damage extent and be used for damage extent identification.

$$RNS_i = NDV_i^S \times \alpha_S$$
$$RNV_i = NDV_i^V \times \alpha_V \tag{9}$$

$$\alpha_S = max(Z_S) - min(Z_S)$$
$$\alpha_V = max(Z_V) - min(Z_V) \tag{10}$$

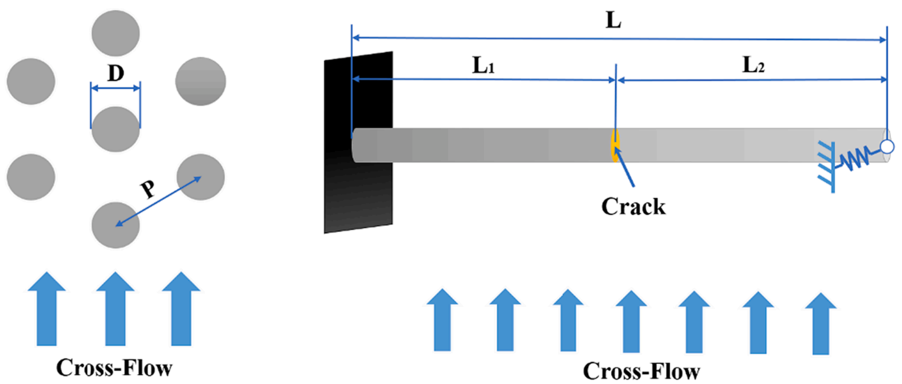

Fig. 2. The tube model.

3. Case study

3.1. Model information

To investigate the effectiveness of the proposed method, the vibration responses of a flexible tube in a rotated triangular tube array with a crack subjected to cross-flow and loose support were calculated for three flow pitch velocity conditions. In the calculation, the finite difference solution was adopted to divide the cracked tube into 59 elements with 60 nodes, as shown in Fig. 2. The influences of the crack position on the tube dynamic responses were investigated.

To simulate the crack damage, the tube is divided into two parts with the same section properties. The dimensionless displacement of the tube with a crack is expressed as:

$$\eta(\xi,\tau)=\begin{cases}\sum_{i=1}^{N_1}\varphi_{1i}(\xi)q_i(\tau) & -L_1\leqslant x<0^-\\ \sum_{i=1}^{N_2}\varphi_{2i}(\xi)q_i(\tau) & 0^+\leqslant x<L_2\end{cases} \tag{11}$$

The corresponding boundary conditions of the two parts are as follows:

$$\begin{aligned}
&x=-L_1:\begin{cases}\varphi_{1i}(-L_1)=0\\ \varphi_{1i}^{'}(-L_1)=0\end{cases}\\
&x=L_2:\begin{cases}\varphi_{2i}^{''}(L_2)=0\\ \varphi_{2i}^{'''}(L_2)=0\end{cases}\\
&x=0:\begin{cases}\varphi_{1i}(0^-)=\varphi_{2i}(0^+)\\ \varphi_{1i}^{''}(0^-)=\varphi_{2i}^{''}(0^+)\\ \varphi_{1i}^{'''}(0^-)=\varphi_{2i}^{''\prime}(0^+)\\ -EI\varphi_{1i}^{''}(0^-)=K_T\left[\varphi_{1i}^{'}(0^-)-\varphi_{2i}^{'}(0^+)\right]\end{cases}
\end{aligned} \tag{12}$$

where L_1 is the length of the left part of the tube, L_2 is the length of the right part of the tube, K_T is the rigidity modulus of the tube at the crack damage position.

In the work, tube mode with single damage is considered in the paper. The details of damage cases are listed in Table 2. For each damage case, results of the flow pitch velocity $U_p = 1.322$ m/s, $U_p = 1.476$ m/s, $U_p = 1.630$ m/s, $U_p = 1.784$ m/s, $U_p = 1.938$ m/s, $U_p = 2.092$ m/s, $U_p = 2.245$ m/s and $U_p = 2.399$ m/s are used. As the flow pitch velocity increases, dynamic characteristic becomes more and more complicated.

3.2. Dynamic response analysis

According to our previous study, it is known that the fluidelastic instability could occur in the transverse direction firstly. Thus, the lateral displacement and velocity responses are used to identify the structural damages. Dynamic responses of Node 20 and 40 of the intact and damaged specimen (Case 2) are shown in Fig. 3. From Fig. 3 (a), it is noted that the displacement and velocity responses of the Node 20 change greatly after the Node 30 is damaged, although there is a distance between the Node 20 and Node 30. And the same phenomenon can also be observed according to Fig. 3 (b). Therefore, the dynamic responses of the intact specimen could not be used as the baseline in the damage identification process. A baseline-free damage identification method is necessary.

3.3. Identification results of damage index AV_i^{RMS}

Index AV_i^{RMS} results of the six cases are shown in Fig. 4. It is seen that the index AV_i^{RMS} could identify the damage location exactly. As the flow pitch velocity increases, the effectiveness of the proposed damage index is always stable, indicating that the proposed damage index could be used in a wide-range flow pitch velocity case.

As the damage location moves from node 10 to node 50, the damage is closer to the loose support and is further from the clamped

Table 2
Damage cases.

	Damage Extent	Damage Location
Case 1	10%	Node 10
Case 2	10%	Node 30
Case 3	10%	Node 50
Case 4	5%	Node 30
Case 5	5%	Node 50
Case 6	2%	Node 50

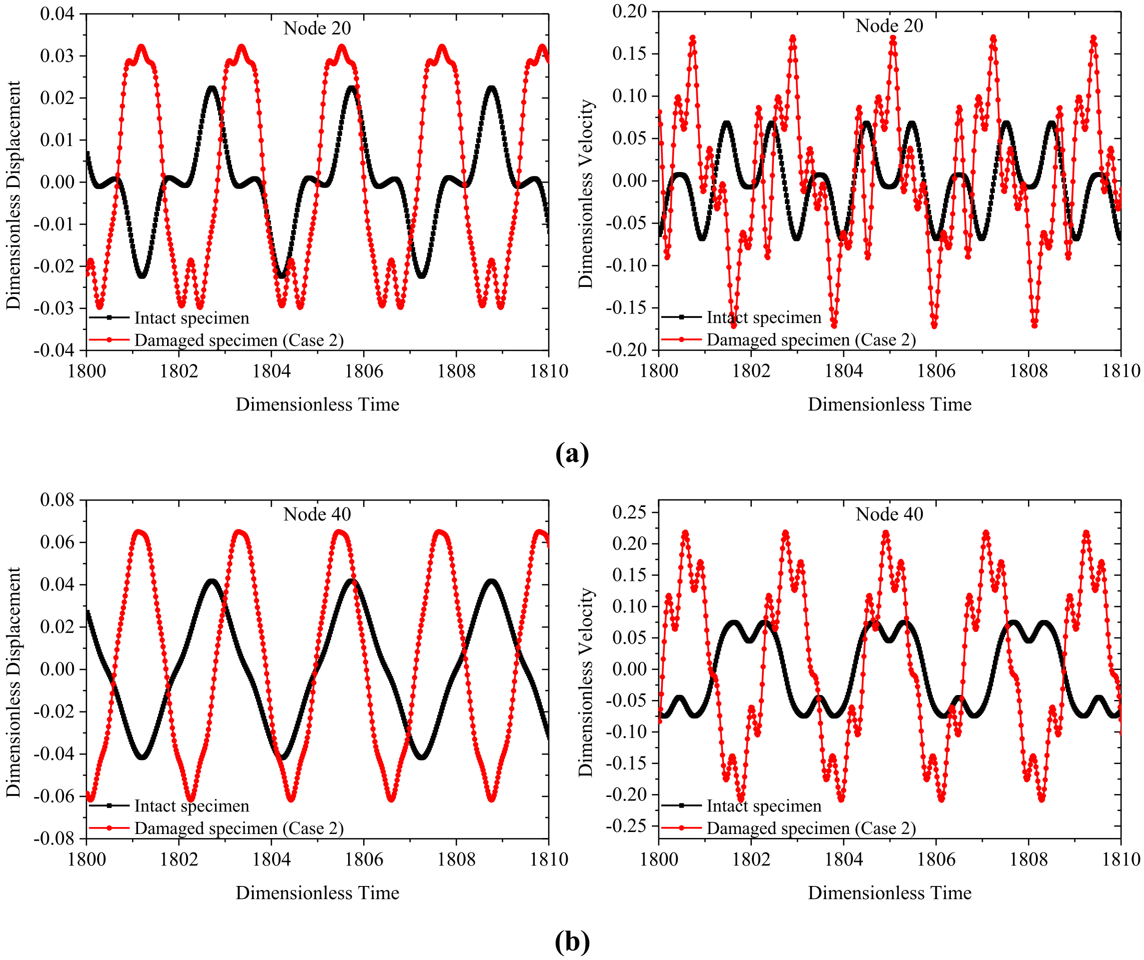

Fig. 3. Displacement and velocity response of (a) Node 20; (b) Node 40.

boundary condition. In previous work, it is easier to identify the damages around the restrained boundary. From Fig. 4 (a) to (c), when the Node 50 is damaged, as the flow pitch velocity increases, the identified results at the damage location are not as good as the results of case 1 and case 2. It reveals that the loose support has influences on the damage identification. Identify the damages close to loose support is harder than identifying the damages close to restrained support. The effect of loose support is discussed in Section 4.1.

Comparing Fig. 4 (b) with (d), as the damage extent decreases, the influence of element 55 becomes more obvious. The same phenomenon could also be obtained from Fig. 4 (c), (e) and (f). Because the velocity and displacement responses are normalized, the results could identify the damage location exactly. However, it could not reflect the damage extent. Therefore, results based on the index 2 is also provided.

3.4. *Identification results of damage index* RV_i^{RMS}

To investigate the effectiveness of index RV_i^{RMS} in damage extent identification, results of Node 30 and Node 50 damaged with extent 2%, 5% and 10% are shown in Fig. 5 and Fig. 6. When Node 30 is damaged (Fig. 5), results in the case of flow pitch velocity 1.938 m/s, 2.092 m/s, 2.245 m/s and 2.399 m/s are provided. It is seen that the damage index RV_i^{RMS} increases as the damage extent increases from 2% to 10%.

When Node 50 is damaged, the results are provided in Fig. 6. When the flow pitch velocity is low, index RV_i^{RMS} can identify both damage location and damage extent. However, when the flow pitch velocity is high, the damage extent could not be identified accurately. It may be because the nonlinear vibration property increases as the flow pitch velocity increases, causing the damage identification more difficult.

For the six cases, the results of damage index $\boldsymbol{RV_i^{RMS}}$ are provided in Fig. 7. As the flow pitch velocity increases, especially when the flow pitch velocity is more than 2 m/s, index $\boldsymbol{RV_i^{RMS}}$ changes greatly. The relationship between index $\boldsymbol{RV_i^{RMS}}$ and flow pitch velocity is not linear and complicated, which demonstrates that the flow pitch velocity has a great influence on the damage feature identification and make the damage identification more difficult.

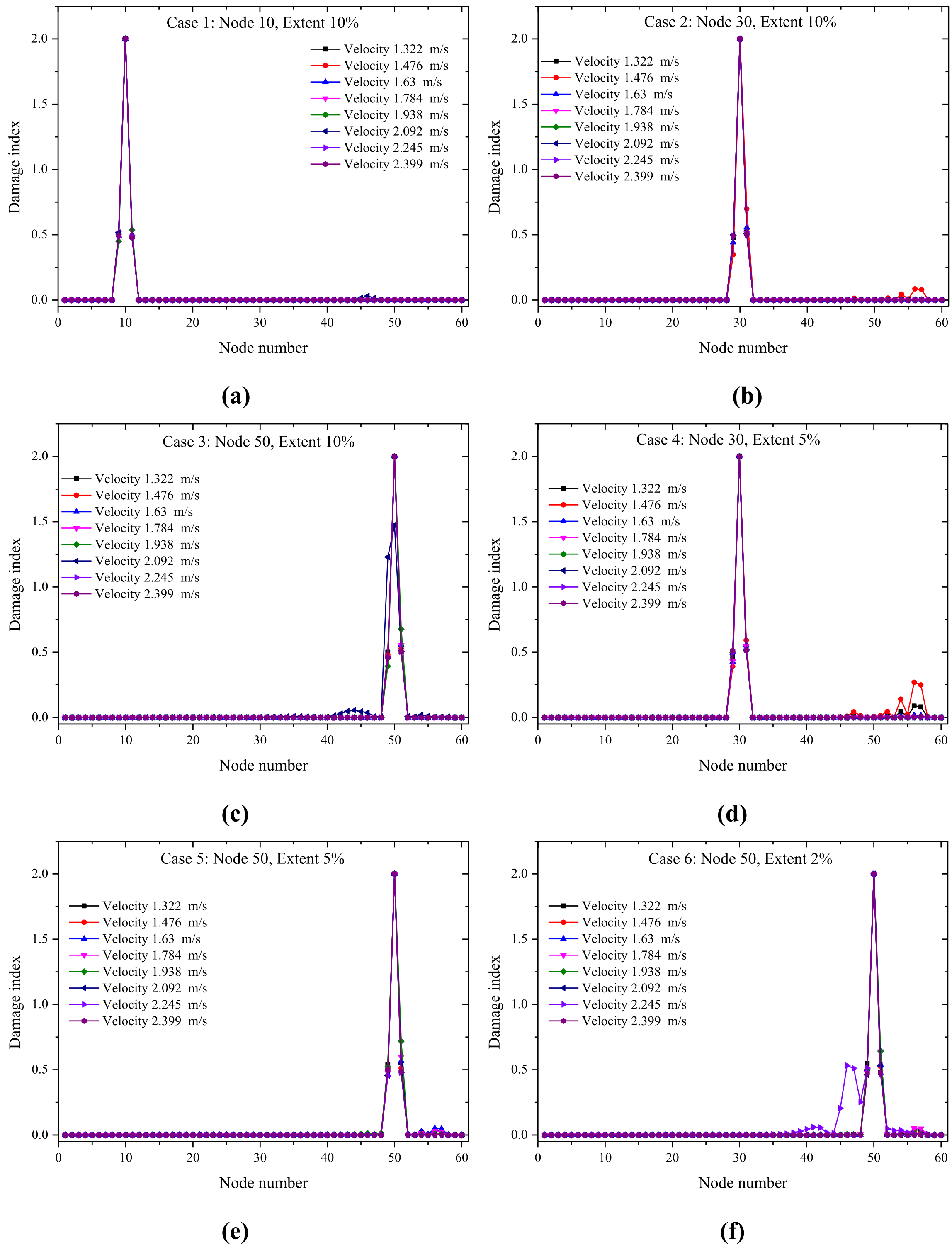

Fig. 4. Results of index AV_i^{RMS}. (a) ~ (f): Case 1 ~ Case 6.

4. Discussion

The proposed method is based on structural dynamic response, which is affected by the many factors, such as the boundary condition and the number of measure points, and so on. To investigate the effectiveness of the proposed method, the influences of two

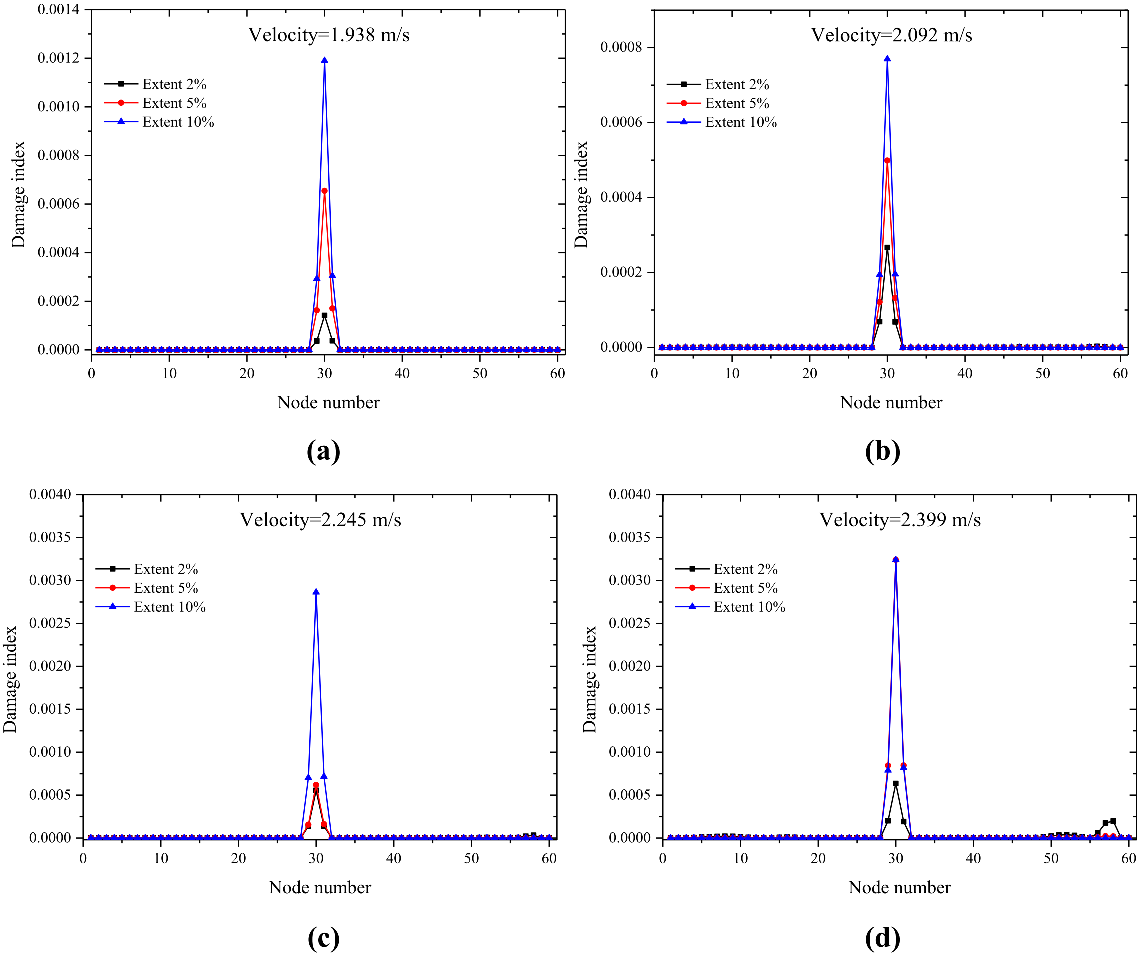

Fig. 5. RV_i^{RMS} results for Node 30 damaged. (a) $U_p = 1.938$ m/s. (b) $U_p = 2.092$ m/s. (c) $U_p = 2.245$ m/s. (d) $U_p = 2.399$ m/s.

factors, loose support location and the number of measure points, are discussed in this section.

4.1. *Effect of loose support location*

Loose support may induce the strong nonlinear dynamic properties, causing structural damage identification more difficulty. The response of Node 50 in the case of the loose support at Node 45 and 60 are provided in Fig. 8. It is seen that the structural dynamic responses (both amplitude and frequency domain characteristics) change a lot when the loose location moves from Node 45 to Node 60.

When Node 30 is damaged with extent 5%, results with loose location Node 45 is provided in Fig. 9. Results in the case of different flow pitch velocities are calculated. When the loose location is at Node 45, two peaks will appear as the flow pitch velocity increases. When the flow pitch velocity is less than 1.784 m/s, there is only one peak caused by the damage, as shown in Fig. 9 (a) and (b). However, when the flow pitch velocity is larger than 1.938 m/s, there are two peaks, as Fig. 10 shown. One is caused by the damage, and the other peak may be caused by the loose support. As the flow pitch velocity increases, the second peak gets closer to the loose support Node 45.

When the Node 50 is damaged and the loose support location is Node 45, the similar phenomenon can be obtained from Fig. 11. When the flow pitch velocity is larger than 1.938 m/s, another peak appears. As the flow pitch velocity increases, the second peak gets closer to the loose support Node 45.

From Fig. 9, Fig. 10 and Fig. 11, it is found that the loose support location plays an important role in the damage identification. It effects the accuracy of damage identification greatly as the flow pitch velocity increases. When damage is at Node 30 or Node 50, the proposed method is effective when the flow pitch velocity is less than 1.938 m/s.

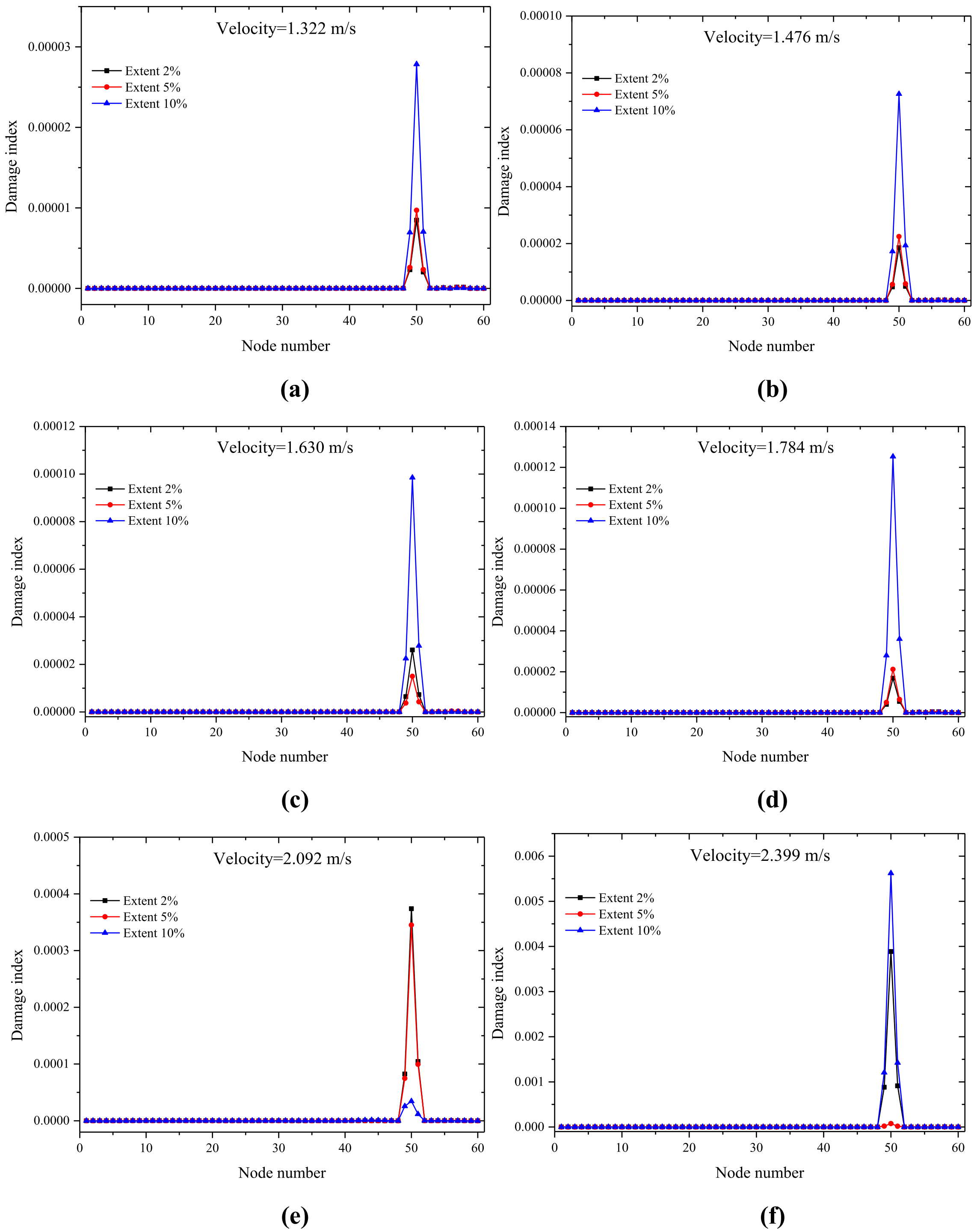

Fig. 6. RV_i^{RMS} results for Node 50 damaged. (a) $U_p = 1.322$ m/s. (b) $U_p = 1.476$ m/s. (c) $U_p = 1.630$ m/s. (d) $U_p = 1.784$ m/s. (e) $U_p = 2.092$ m/s. (f) $U_p = 2.399$ m/s.

4.2. Effect of number of measure points

As we know, in the actual measurements, the number of measure points is limited. In section 3, 60 measure points are used. In this section, 30 measure points are used. When Node 30 and Node 50 are damaged, results in the cases of extent 10%, 5%, 2% and $U_p = 1.322$ m/s and $U_p = 12.245$ m/s are provided in Fig. 12.

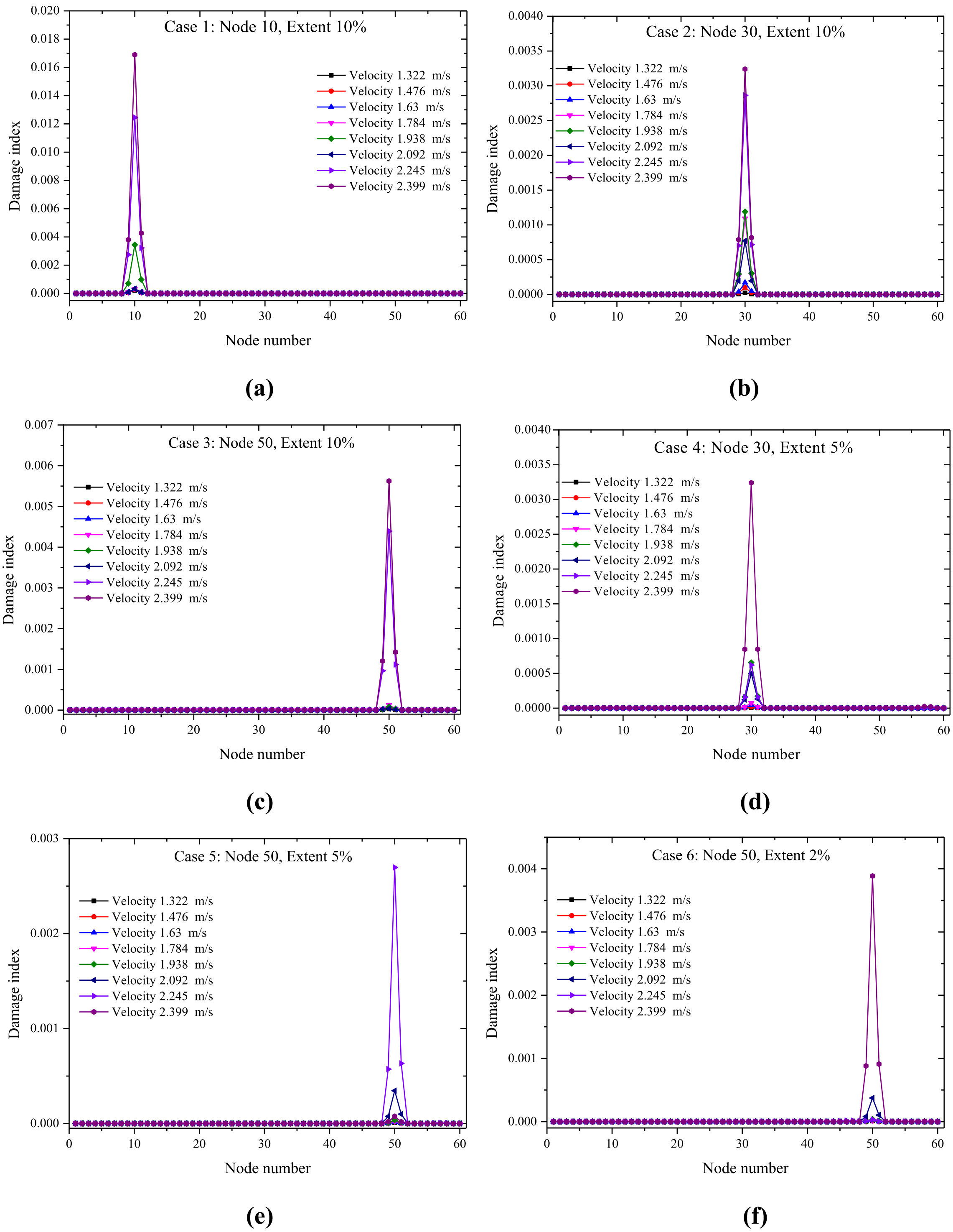

Fig. 7. RV_i^{RMS} results. (a) ~ (f): Case 1 ~ Case 6.

From Fig. 12 (a) and (b), when the extent is 5% or 10%, index $\boldsymbol{AV_i^{RMS}}$ could identify the damage location in the case of 30 measure points. When the extent is 2%, there are also some small peaks caused by non-damage factors, affecting the identification of the real damage Node 30.

From Fig. 12 (c) and (d), when Node 50 is damaged and the flow pitch velocity is 1.322 m/s, index $\boldsymbol{AV_i^{RMS}}$ could identify the damaged Node 50 very effectively. However, when the flow pitch velocity is 2.245 m/s and extent is 2%, there are some small peaks

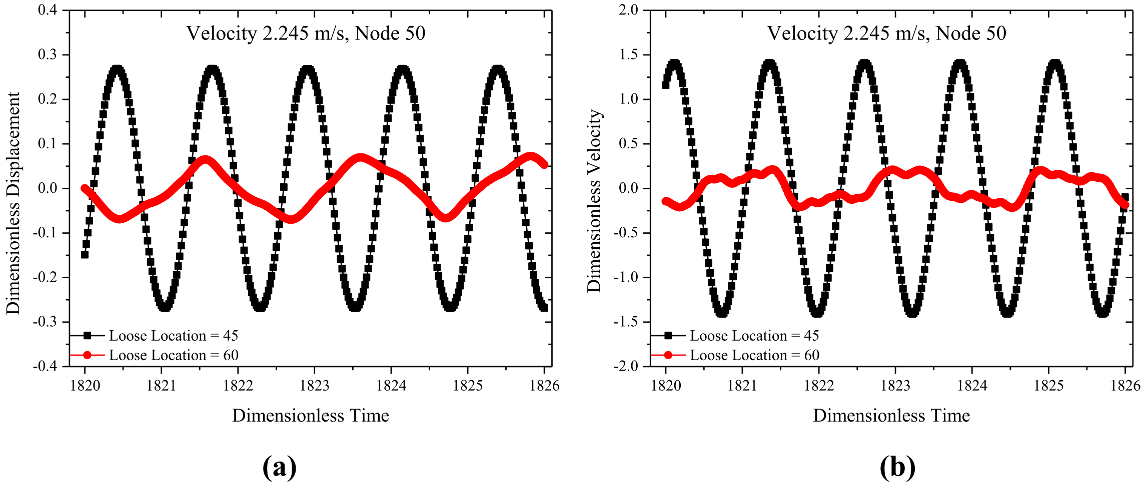

Fig. 8. Responses of Node 50 in the case of $U_p = 2.245$ m/s. (a) Displacement. (b) Velocity.

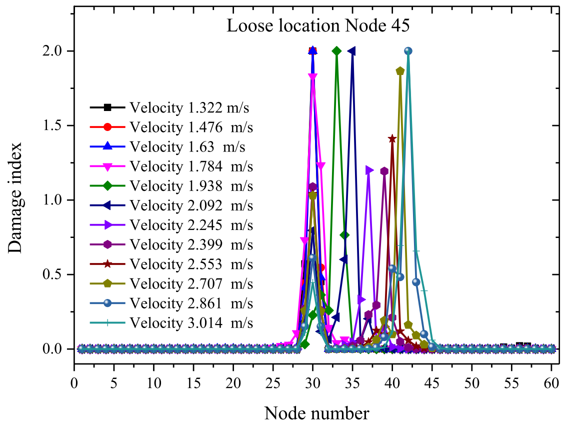

Fig. 9. Results for Node 30 damaged with loose location Node 45 and extent 5%.

around the real damage, inducing the accuracy of the damage localization decreasing.

When the measure points decreases, the effectiveness of the proposed method is affected. When the damage extent is not less than 5%, the proposed method is still very effective. When the damage extent is 2%, the effectiveness of the method is affected in some extent.

5. Conclusion

In this paper, a baseline-free method is proposed for identifying damages of tube bundles subjected to cross-flow and loose support. Two damage indexes, index AV_i^{RMS} and index RV_i^{RMS} are used to identify the damage location and extent. Effect of the flow pitch velocity, loose support location, number of measure points on the effectiveness of the proposed method are discussed. Some conclusions are listed:

(1) The proposed damage index AV_i^{RMS} can identify the damage location accurately. The smallest identified damage extent is 2%.
(2) The proposed index RV_i^{RMS} can identify the damage extent when the flow pitch velocity is small. When the flow pitch velocity is large, the effectiveness of index RV_i^{RMS} decreases.
(3) The loose support location has an influence on the effectiveness of the proposed method, especially when the flow pitch velocity is large.
(4) When the damage extent is small, the number of measure points has a little influence on the method. When the damage extent is large, the effect of number of measure points decreases.

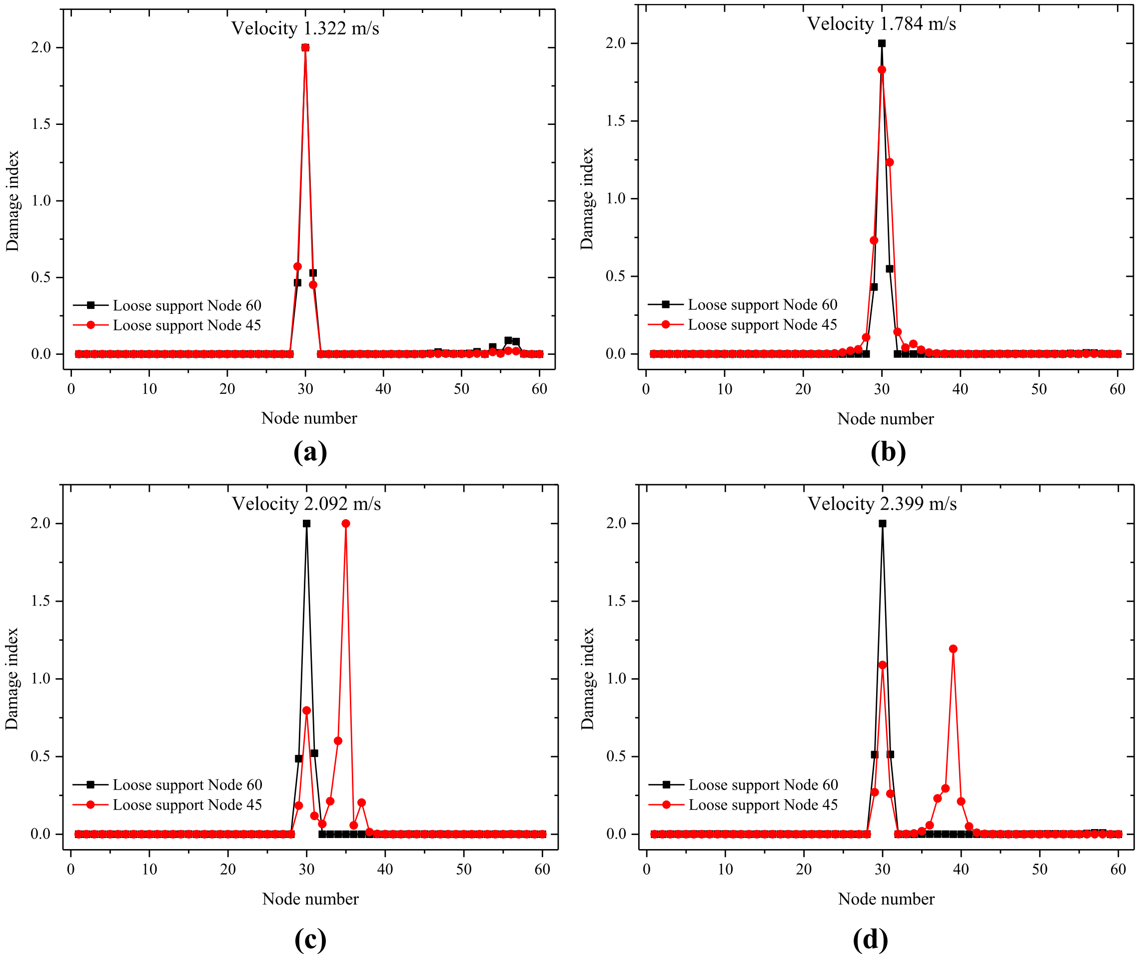

Fig. 10. Results in the case of different loose locations. (a) $U_p = 1.322$ m/s. (b) $U_p = 1.784$ m/s. (c) $U_p = 2.092$ m/s. (d) $U_p = 2.399$ m/s.

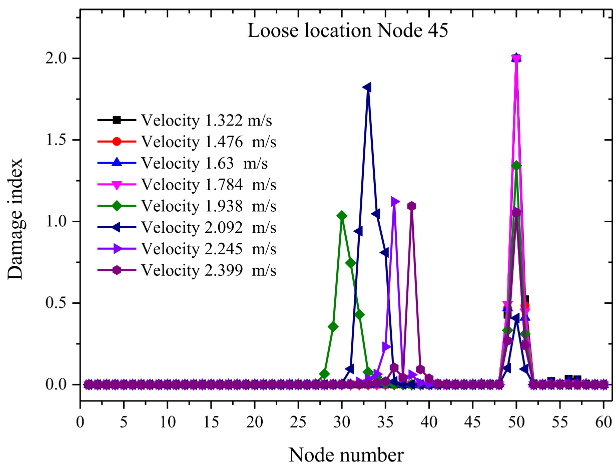

Fig. 11. Results for Node 50 damaged with loose location Node 45 and extent 5%.

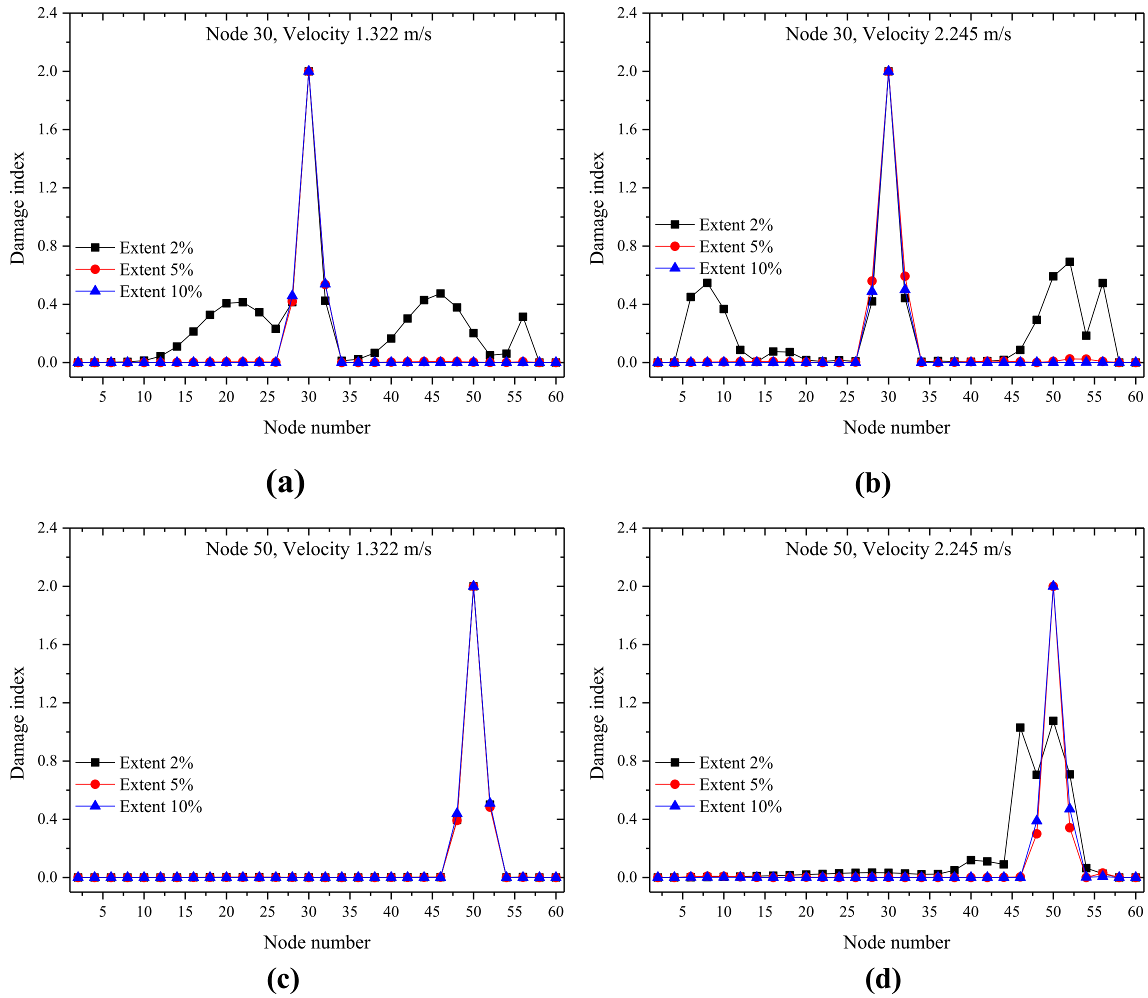

Fig. 12. Effect of sensors number. (a) Node 30, $U_p = 1.322$ m/s. (b) Node 30, $U_p = 2.245$ m/s. (c) Node 50, $U_p = 1.322$ m/s. (d) Node 50, $U_p = 2.245$ m/s.

CRediT authorship contribution statement

Lingling Lu: Methodology, Funding acquisition. **Jiang Lai:** Conceptualization, Funding acquisition. **Shihao Yang:** Writing - review & editing. **HW Song:** Supervision. **Lei Sun:** Supervision.

Declaration of Competing Interest

The authors declare that they have no known competing financial interests or personal relationships that could have appeared to influence the work reported in this paper.

Acknowledgments

This research is supported by the National Natural Science Foundation of China (Grant Nos. 11972033 and 12072336), and the Strategic Priority Research Program of the Chinese Academy of Sciences (Grant No. XDA22000000).

References

[1] J. Lai, L. Sun, P. Li, Two-phase flow-induced instability and nonlinear dynamics of a single tube in tube bundles in the transverse direction, European Journal of Mechanics/ A solid 78 (2019) 103858, https://doi.org/10.1016/j.euromechsol.2019.103858.

[2] Y. Joo, V.K. Dhir, On the mechanism of fluidelastic instability of a tube placed in an array subjected to two-phase crossflow, J. Fluids Eng. 117 (4) (1995) 706–712.

[3] S.S. Chen, Y. Cai, G.S. Srikantiah, Fluid damping controlled instability of tubes in crossflow, J. Sound Vib. 217 (5) (1998) 883–907.

[4] J.P. Noel, G. Kerschen, Nonlinear system identification in structural dynamics: 10 more years of progress, Mech. Syst. Sig. Process. 83 (2016) 2–35.

[5] L. Wang, X. Zhou, H.e. Liu, W. Yan, Damage detection of RC beams based on experiment and analysis of nonlinear dynamic characteristics, Constr. Build. Mater. 29 (2012) 420–427.
[6] M. Kumar, R.A. Shenoi, S.J. Cox, Experimental validation of modal strain energies based damage identification method for a composite sandwich beam, Compos. Sci. Technol. 69 (10) (2009) 1635–1643.
[7] S. Tian, Z. Chen, L. Chen, D. Zhang, Numerical analyses on influence of damage configuration on vibration parameters for lattice sandwich plate, Int. J. Appl. Electromagnet Mech 33 (3-4) (2010) 1565–1572.
[8] K. Zhu, M. Chen, Q. Lu, B.o. Wang, D. Fang, Debonding detection of honeycomb sandwich structures using frequency response functions, J. Sound Vib. 333 (21) (2014) 5299–5311.
[9] S.B. Shiki, S. da Silva, M.D. Todd, On the application of discrete-time Volterra series for the damage detection problem in initially nonlinear systems, Structural Health Monitoring 16 (1) (2017) 62–78.
[10] L.N. Virgin, Introduction to Experimental Nonlinear Dynamics, Meas. Sci. Technol. 12 (3) (2001) 52.
[11] S.L. Tsyfansky, V.I. Beresnevich, Non-linear vibration method for detection of fatigue cracks in aircraft wings, J. Sound Vib. 236 (2000) 9–60.
[12] S. Benfratello, P. Cacciola, N. Impollonia, A. Masnata, G. Muscolino, Numerical and experimental verification of a technique for locating a fatigue crack on beams vibrating under Gaussian excitation, Eng. Fract. Mech. 74 (18) (2007) 2992–3001.
[13] V.K. Nguyen, O. Olatunbosun, A proposed method for fatigue crack detection and monitoring using the breathing crack phenomenon and wavelet analysis, Journal of Mechanics of materials and structures 2 (3) (2007) 399–420.
[14] F. Léonard, J. Lanteigne, S. Lalonde, Y. Turcotte, Free-vibration behaviour of a cracked cantilever beam and crack detection, Mech. Syst. Sig. Process. 15 (3) (2001) 529–548.
[15] E. Douka, L.J. Hadjileontiadis, Time–frequency analysis of the free vibration response of a beam with a breathing crack, NDT and E Int. 38 (1) (2005) 3–10.
[16] C.R. Farrar, K. Worden, M.D. Todd, Nonlinear system identification for damage detection, Los Alamos National Laboratory, Los Alamos NM, 2007.
[17] R.P. Bandara, T.HT. Chan, D.P. Thambiratnam, Structural damage detection method using frequency response functions, Structural Health Monitoring 13 (4) (2014) 418–429.
[18] N.P. Yelve, M. Mitra, P.M. Mujumdar, Spectral damage index for estimation of breathing crack depth in an aluminum plate using nonlinear Lamb wave, Structural Control and Health Monitoring 21 (5) (2014) 833–846.
[19] L. Bornn, C.R. Farrar, G. Park, Damage detection in initially nonlinear systems, Int. J. Eng. Sci. 48 (10) (2010) 909–920.
[20] M. Jiang, W. Zhang, Q. Lu, A nonlinearity measure-based damage location method for beam-like structures, Measurement 146 (2019) 571–581.
[21] L.G.G. Villani, S.d. Silva, A. Cunha, Damage detection in an uncertain nonlinear beam, Procedia Eng. 199 (2017) 2090–2095.
[22] B. Bhowmik, T. Tripura, B. Hazra, V. Pakrashi, Robust linear and nonlinear structural damage detection using recursive canonical correlation analysis, Mech. Syst. Sig. Process. 136 (2020) 106499, https://doi.org/10.1016/j.ymssp.2019.106499.
[23] J. Lai, L. Lu, S. Yang, T. Tan, L. Sun, Dynamic characteristics of tube bundles with crack subjected to cross-flow and loose support, Appl. Math. Model. (2021) under review.
[24] C.P. Ratcliffe, Damage detection using a modified laplacian operator on mode shape data, J. Sound Vib. 204 (3) (1997) 505–517.
[25] M.K. Yoon, D. Heider, J.W. Gillespie, C.P. Ratcliffe, R.M. Crane, Local damage detection using the two-dimensional gapped smoothing method, J. Sound Vib. 279 (1-2) (2005) 119–139.